

## AERODYNAMIC CHARACTERISTICS OF TRANSPORT AIRPLANES IN LOW SPEED CONFIGURATION

R. Martínez-Val\*, T. Muñoz+, E. Pérez" and J. Santo-Tomás+

ETSI Aeronáuticos  
Universidad Politécnica de Madrid  
Madrid, Spain

### Abstract

A prediction method to determine, at preliminary design level, the aerodynamic characteristics of transport airplanes in low speed configuration has been developed. Starting from the aerodynamic data of a clean configuration, that are assumed to be known, the method provides the corresponding increases in lift, drag and pitching moment due to deployment of leading edge or trailing edge high lift devices (separately or in combination) in a three step procedure: two dimensional variations, complete wing and complete airplane.

The analysis of two dimensional cases is carried out by means of semiempirical models, similar to those ones reported in literature, but specifically adapted to aft-loaded airfoils; such feature was an initial requirement for this work. Lifting surface theory is used to compute lift, induced drag and pitching moment of the wing, whose airfoil sections and high lift devices may change along the spanwise direction in discrete steps. All important geometrical and aerodynamic variables are considered: wing sweep, thickness, taper, twist, etc. Raw data are smoothed of spanwise discontinuities effects. Parasite drag is obtained integrating and correcting the appropriate values of 2D sections. Classical flight mechanics relations are used to determine the aerodynamic characteristics of the complete airplane, paying special attention to downwash effects at the horizontal tail.

### Introduction

The objective of present work is to compute, within the accuracy required at preliminary design level, the variation of aerodynamic characteristics of airplanes due to deployment of high lift devices. It is assumed that the properties of the original clean configuration are known.

Aircraft aerodynamics is very important along the design process, remarkably in the initial phases, due to its impact on performances, stability and control characteristics.

There are four types of methods to predict the aerodynamic behaviour at low speed<sup>1</sup>: three-dimensional analytical methods, of diverse complexity, that may include real flow effects such as boundary layers, turbulence, etc<sup>2-5</sup>; two dimensional analytical techniques, mainly used for calculating potential and viscous flows around multi-element airfoils or to design new airfoil shapes<sup>6-11</sup>; empirical and semiempirical methods to estimate variables that are difficult to obtain by means of analytical treatments, like maximum lift coefficient,<sup>12,13</sup> and carefully performed wind tunnel experiments.<sup>14,15</sup>

From the viewpoint of the design phases a different scheme can be envisaged, as shown in Table 1, taking into account time and cost. According to this scheme, the preliminary design phase is better fitted to semiempirical methods, adapted for the particular aspects to be covered in each study. In the compromise between accuracy in one hand and time-cost on the other they have clear advantages<sup>16</sup>, in a period of quick changes and evolving configuration.

It is important to notice that numerical methods usually require the support of wind tunnel measurements to adjust the parameters appearing in the corresponding algorithms; in the other hand, however, empirical methods are only useful for known geometries and can hardly help in the development of new concepts.

The difficulty of theoretical studies comes from the detailed actual geometry and the complexity of the flow around actual wings with high lift devices, because of the presence of severe discontinuities in the spanwise lift distribution, as shown in Fig. 1. Such discontinuities have pernicious effects that increase the total induced drag in low speed configuration. In real world and in modelling this can be partially compensated; for example, using the inner ailerons as flaps.

Most numerical methods have been developed and adapted to the detailed design phase, since they require a very precise knowledge of airfoil or wing geometry: actual flow paths, gaps, etc. Only the inverse methods are adequate to iterate between some aerodynamic objectives and an unknown geometry<sup>17-19</sup>.

Literature provides a range of errors corresponding to different methods. Both empirical and simple numerical treatments are in the order of 5-10%, that are acceptable for preliminary design. For example, the accuracy in estimating

\* Professor of Aircraft Design, Member AIAA

" Associate Professor, Aircraft Design

+ Lecturer, Aircraft Design

ETSI Aeronauticos  
Plaza Cardenal Cisneros, 3  
28040 Madrid, Spain

Copyright © 1992 by the American Institute of Aeronautics and Astronautics, Inc. and the International Council of the Aeronautical Sciences. All rights reserved.

TABLE 1. Prediction methods in airplane design

Level of design	Accuracy	Computing time	Type of method	Type of computer
Conceptual	7-15%	negligible	empirical	calculator
Preliminary	5-10%	very low	semi-emp.	personal
Detailed	1-5%	reasonable	analytical	main frame

the maximum lift coefficient is around 0.1 or 0.2. But the ability to predict drag (friction and profile) is very poor<sup>20-22</sup> and the same can be said about pitching moment<sup>4,20,23</sup> although the least deviations will correspond to small angles of attack and small high lift device deflections.

With small angle of attack and small high lift device deflection the accuracy of empirical and simple numerical methods is about the same. However, when approaching more complex flow situations these last ones are preferred for their advantage in accuracy and minimum time-cost required.

The particular procedure described here has been developed under contractual agreement with the Preliminary Design Department of Construcciones Aeronauticas S.A. (CASA). Initial specifications indicated that the method should consider complete wing configurations; and be specially adapted to aft loaded airfoils, and for some specific high lift devices: plain flaps, single and double slotted Fowler flaps, slats and Krueger flaps.

#### Description of the model

After a detailed review of literature on the topic and analysis of the different existing approaches for estimating the afore mentioned aerodynamic characteristics, the following scheme has been adopted. First, the attention is concentrated in two-dimensional configurations, i.e. airfoils with high-lift devices, and their characteristics are determined using semiempirical methods similar to those described in ESDU<sup>12</sup>, Roskam<sup>13</sup>, Torenbeek<sup>24</sup>, etc; data to adjust mathematical expressions are mostly taken from NASA Reports and other bibliographical sources publishing experimental results on aft loaded airfoils. The three-dimensional section uses a lifting surface method to generate the loading along the wing span providing, accordingly, lift, pitching moment and induced drag coefficients for the complete wing; the parasite drag is again computed by means of empirical methods, integrating the properties of different wing sections. The last section of the model, based on classical Flight Mechanics equations and some empirism, gives the complete airplane behaviour.

It must be recalled that the precise characteristics with high lift devices deployed depend strongly on geometrical peculiarities (gaps, overlaps, etc) that should finally be studied and refined in wind tunnel tests<sup>16</sup> or with more accurate methods in later phases of the design.

From the many existing high lift devices, only slats and Krueger flaps in the leading edge and plain flaps and Fowler flaps in the trailing edge have been considered,

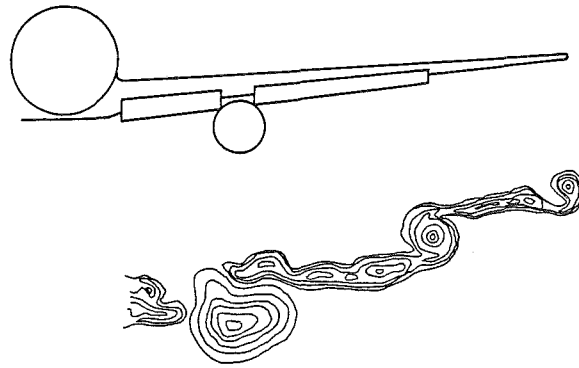


FIGURE 1. Sketch of airplane in low speed configuration and downstream flow.

according to the afore mentioned contractual agreement with CASA. Because of confidentiality reasons, only global expressions will be presented here.

#### Two-dimensional sections

The important variables of present study, whose variations have to be computed, are: lift at zero angle of attack; lift curve slope; maximum lift; angle of attack for maximum lift; minimum parasite drag; lift at which minimum parasite drag is achieved; change of drag with respect to lift; pitching moment at zero angle of attack; change of pitching moment with lift. That is, a total of nine variables.

Lift of plain flaps has been derived from ESDU<sup>12</sup> formulations with only some minor modifications, since those results are essentially valid for aft loaded airfoils. In its turn, the expressions for Fowler flap, taken from Roskam<sup>13</sup>, needed some refinements; particularly to account for chord extension<sup>20,24</sup> and equivalent deflection in double slotted Fowler flaps<sup>14,25,26</sup>. In all cases the increase in lift at zero angle of attack can be expressed as

$$\Delta Cl_o = Cl_\alpha \alpha_\delta \delta_f \frac{c'}{c} \quad (1)$$

where  $\alpha_\delta$  is an efficiency factor that depends on the deflection angle, flap chord ratio and relative thickness of the airfoil.

The chord extension ratio,  $c'/c$ , appearing in Eq. (1) is also used as an increase factor in the lift curve slope<sup>13,23,24</sup>. Maximum lift is computed with the corresponding correction factors that include, for example, the leading edge curvature in the case of plain flaps,  $\rho_l$ , as shown in Eq. (2). As stated above the detailed mathematical expressions are confidential.

$$\Delta Cl_{max} = f(Re, \rho_l, \delta_f, \frac{c'}{c}) \Delta Cl_o \quad (2)$$

The aerodynamic characteristics of airfoils with leading edge devices have been determined following ESDU<sup>12</sup> indications. The chord extension ratio of slats is computed according to a circular arc extension mechanism,

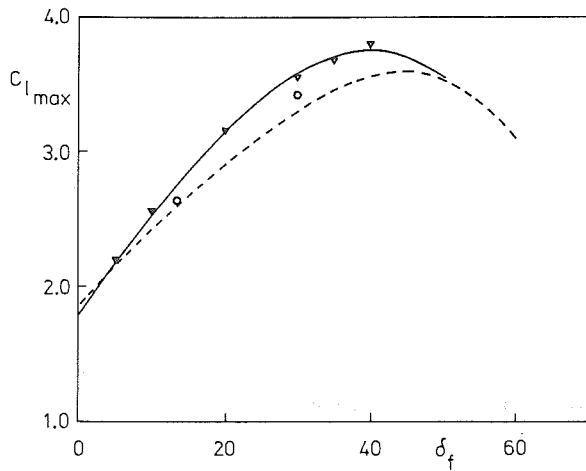


FIGURE 2. Prediction of  $C_{l_{max}}$  for airfoil ( $t/c=0.17$ ) with Fowler flap (solid line) and double slotted Fowler flap ( $t/c=0.09$ ; dashed line) with corresponding experimental data; triangles and circles, respectively.

similar to the one used in existing airplanes. The deflection angles of slats and Krueger flaps are defined according to their different geometries.

Appropriate correction factors have been applied to the case of simultaneous deployment of leading edge and trailing edge devices, following closely again the indications of afore mentioned empirical methods. It can be argued that in simultaneous deployment the equivalent chord is

$$c' = c + \Delta c_f + \Delta c_t \quad (3)$$

and since lift increase depend upon  $c'/c$ , all contributions must be recalculated for the new ratio. After that,

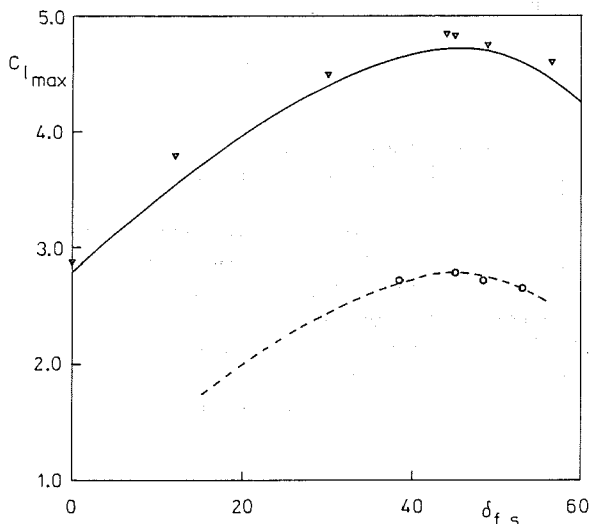


FIGURE 3. Prediction of  $C_{l_{max}}$  for airfoil with slat (dashed line) and airfoil with slat and double slotted Fowler flap, with corresponding experimental data.

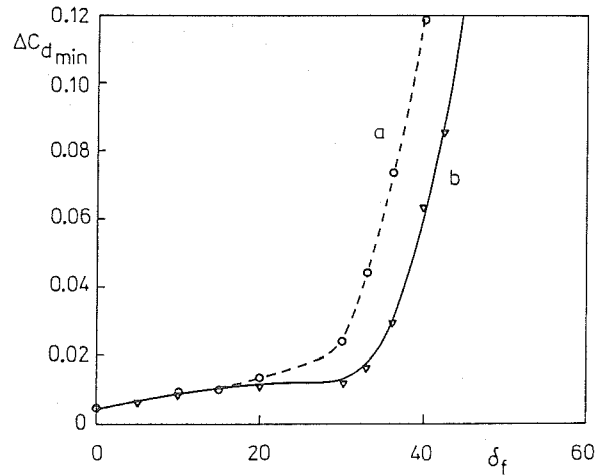


FIGURE 4. Prediction of increase in minimum drag of conventional (dashed line) and aft loaded airfoils (solid line) with Fowler flaps.

$$\Delta C_{l_o} = \Delta C_{l_{o_f}} + \Delta C_{l_{o_t}} \quad (4)$$

$$\Delta C_{l_{max}} = \Delta C_{l_{max_f}} + \Delta C_{l_{max_t}} - \Delta C_{l^*} \quad (5)$$

The small decrease at the end of Eq. (5) is equivalent to a loss of some few degrees of angle of attack.

Some of the data reported in literature were used to adjust the parameters appearing in diverse expressions of the method, and some others to evaluate the accuracy of two-dimensional estimations of lift. Figures 2 and 3 depict several comparisons in different airfoil-high lift device configurations, showing always very good agreement; in some cases without measurable error, or in the conservative side.

There are several empirical methods reported in literature to estimate drag in two-dimensional configurations, with noticeable similarities to each other. However, some important variables are not included or its functional dependence is not properly expressed for aft loaded airfoils. A common expression has been used for the two-dimensional polar

$$Cd = Cd_{min} - p (Cl - Cl_{md})^2 \quad (6)$$

Consequently, three different parameters must be computed for each configuration.

Completely new expressions have been developed for plain and Fowler flaps. Minimum parasite drag can be determined in terms of thickness to chord ratio, flap chord ratio and deflection angle. Typical results appear in Fig. 4, showing the different behaviour of distinct airfoil types. It seems to exist a technological factor that produces such effect. In the case of double slotted Fowler flaps a deflection larger than the equivalent one must be used, due to the particular geometry of this flap.

Data reported in literature indicate that the polar curvature,  $p$ , is not changed by trailing edge flap deflections; and the lift at which minimum parasite drag is achieved can be expressed as<sup>24</sup>

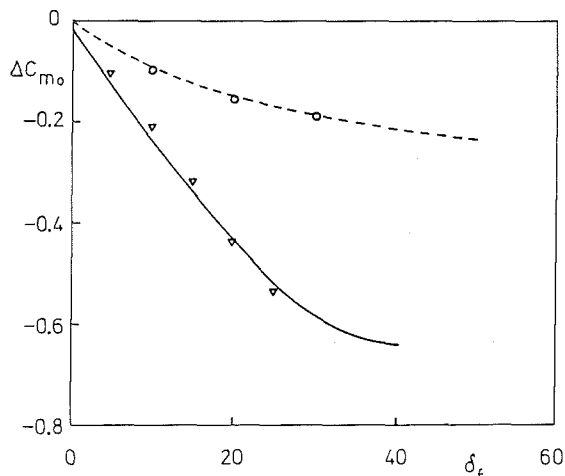


FIGURE 5. Variation of pitching moment due to the deployment of plain flap (dashed line) or Fowler flaps (solid line).

$$C_{l_{md}} = C_{l_o} + \frac{\Delta C_{l_o}}{2} \quad (7)$$

Leading edge devices as well as simultaneous trailing edge-leading edge devices have also needed specific treatments, yielding new complex expressions with influence of device chord ratios, deflections and aerodynamic characteristics of the base airfoil.

Pitching moment estimations pose some peculiar difficulties since, in one hand, pitching moment depends strongly on the specific pressure distribution along the airfoil chord and, in the other, a precise position is needed to compute such moment; following the common approach this point was fixed at  $c/4$  although, perhaps, it is not representative of the aerodynamic centre in Fowler flaps.

Two parameters have been selected to describe pitching moment variations: increase of pitching moment coefficient at zero angle of attack, due to deflection of high lift device; and partial derivative with respect to lift within the range of interest (from zero angle of attack to around 75% of maximum lift). Torenbeek<sup>24</sup> and Roskam<sup>13</sup> formulations have been used, with minor modifications, for trailing edge and leading edge devices, respectively; again, the parameters and variables used to compute  $\Delta C_{m_o}$  are the flap chord ratio, full chord extension ratio, deflection of device, lift coefficient at zero angle of attack and  $\Delta C_{l_o}$  due to the particular device. Figure 5 exhibits the comparison with published data. A proper method has been developed for the case of simultaneous deflections.

Not any method has been found in literature that may adequately explain the behaviour of the dependence of pitching moment versus lift, for the particular aft loaded airfoils of present study. Therefore, again, specific expressions have been derived for the diverse cases considered. The main independent variable is the chord extension ratio,  $c'/c$ ; the equivalent chord being a function of device chord ratios and deflections. Figure 6 shows predictions for four different configurations.

The behaviour of plain flap and slat (alone) are easy to understand. Fowler flaps exhibit a peculiar evolution: up

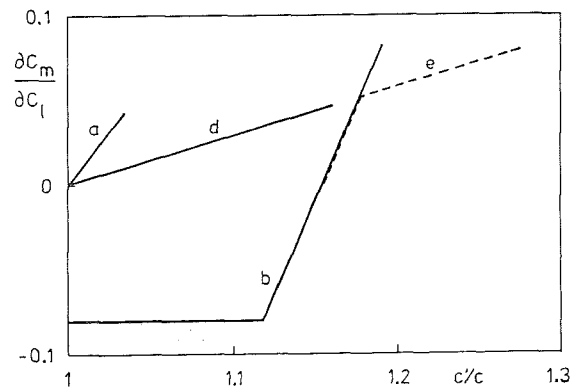


FIGURE 6. Variation of the pitching moment dependence with respect to lift,  $dC_m/dC_l$ , for plain flap (a), Fowler flap (b), slat (d) and simultaneous slat and Fowler flap deployment (e).

to certain chord extension ratio the parameter  $dC_m/dC_l$  keeps its value, and after this threshold evolves like the afore mentioned ones. If a slat and a Fowler flap are deployed simultaneously the evolution coincides with the one corresponding to Fowler flap alone up to the point where the parameter reaches the value of slat alone, following this last behaviour from that point onwards.

#### Complete wing

The objective of the three dimensional integration is to provide lift, drag and pitching moment coefficients of a complete wing, taking into account the wing planform and twist, the properties of airfoil sections and different settings of high lift devices.

It is clear that empirical methods need a large amount of matchings and corrections, due to the numerous possible combinations among variables and parameters<sup>3,27,28</sup>. On the opposite side, analytical treatments can provide fairly accurate results, at least on some of the variables of interest.

The approach considered here is based on the lifting surface theory<sup>29-32</sup>, that provides values of lift, pitching moment and induced drag; leaving parasite drag for a semiempirical final adjustment. Since the scope of the study is restricted to low speed conditions, no compressibility effects are included.

A slightly modified Multhopp's method is used to compute lift and pitching moment at a number of chordwise sections, from a set of linear equations satisfying the conditions at two control points, approximately at  $0.34c$  and  $0.9c$ . The actual wing is discretized into a number of spanwise sections, within which all features except chord are kept uniform, as represented in Fig. 7. The grid for numerical computations is fine enough to reproduce, with adequate accuracy, all spanwise variations of airfoil type and high lift device settings.

The wing is defined by means of the coordinates of several points along leading and trailing edges, that are both then described as two series of straight segments. If the base airfoil of a section has a lift curve slope different

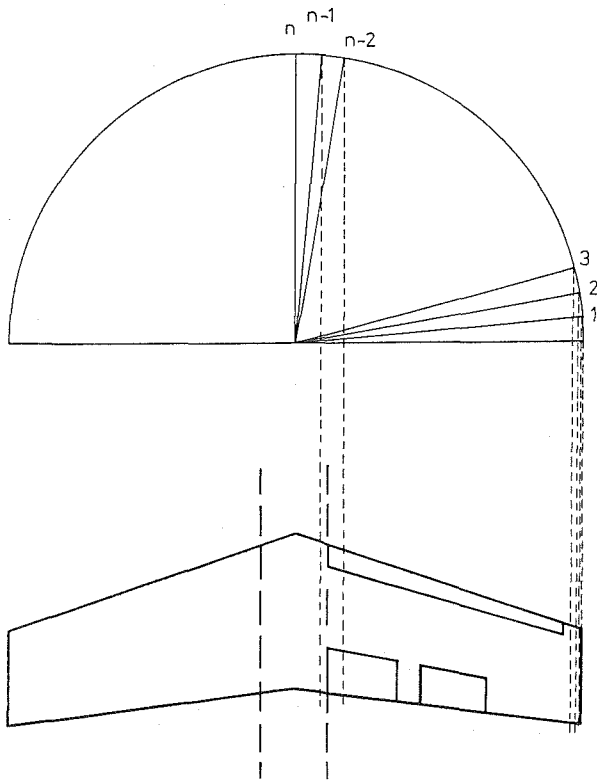


FIGURE 7. Discretization (upper half) and actual planform (lower half) for computations of complete wings.

from  $2\pi$ , the chord at that section is multiplied by  $Cl\alpha/2\pi$ ; after all appropriate changes, the wing planform is ready for the lifting surface method.

Once the spanwise lift distribution is known, the parasite drag of the wing is computed by integration of local parasite drag values, and then added to the induced drag to provide total drag for the particular wing configuration and angle of attack.

Of particular interest is the determination of  $CL_{max}$  for the complete wing. A lift decrease rate is assumed for any wing section that is at an angle of attack higher than the one corresponding to maximum lift. Such rate is large enough to simulate the spread of the stall zone in spanwise direction. According to evaluation tests carried out,  $CL_{max}$  is fairly well defined although the angle of attack at which it is achieved is not so accurately determined. In the other hand, due to the modelling used for 2D airfoil behaviour, drag and pitching moment are computed with lesser accuracy, although this is not an important drawback of the method.

#### Complete aircraft

With respect to the complete aircraft the present study only addresses longitudinal motion, since this is the area of most interest. However, some of the results obtained with the analysis of complete wing could be of some help in non-symmetric cases.

As indicated in the Introduction paragraph, the model described here assumes that all aerodynamic

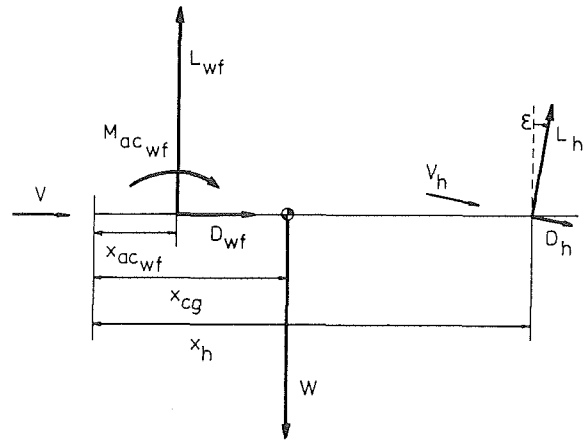


FIGURE 8. System of forces acting on the airplane.

characteristics of the airplane in clean configuration are known; and, therefore, only variations of lift, drag, downwash angle, etc, must be determined.

The balance of forces acting on the airplane (sketched in Fig. 8) provide the following system of equations<sup>13,24,33,34</sup>

$$L_A = L_{wf} + L_h \quad (8)$$

$$D_A = D_{wf} + D_h + L_h \epsilon + D_{ac-wf-h} \quad (9)$$

$$0 = M_{ac_wf} + L_{wf} (x_{cg} - x_{ac_wf}) + L_h (x_{cg} - x_h) \quad (10)$$

Former expressions for lift and pitching moment take only into account effects of wing, horizontal tail and fuselage, since within the accuracy required in this study, other elements have negligible influence. In the other hand, the last term in Eq. (9) includes contributions to drag from fairings, nacelles, protuberances, etc, that are roughly independent of the airplane configuration; i.e. high lift system deployment<sup>2,35</sup>.

Wing-fuselage aerodynamics is determined according to Torenbeek's method<sup>24</sup>, from lift, pitching moment and aerodynamic centre of the wing alone, the geometry of fuselage and the wing-fuselage relative position, with some minor modifications taken from literature<sup>5,33,34,36</sup>. In particular, interference effects of fuselage on flap performance is assumed to be equivalent to having trailing edge devices occupying a larger fraction of the span, augmenting towards wing root.

Downwash on the tail plane is an important matter, mainly for its influence in drag. However, it is difficult to be determined since it depends on local effects, like vortex generators, precise geometry of pylons and nacelles, etc<sup>24,37</sup>. Published methods on downwash estimations are very seldom, commonly using equivalent flow deflection angles that depend on wing planform, type and state of the wake, etc. Even more scarce are the methods that provide the modifications produced by high lift system deployment. In the present work Roskam's method<sup>13</sup> is used due to its

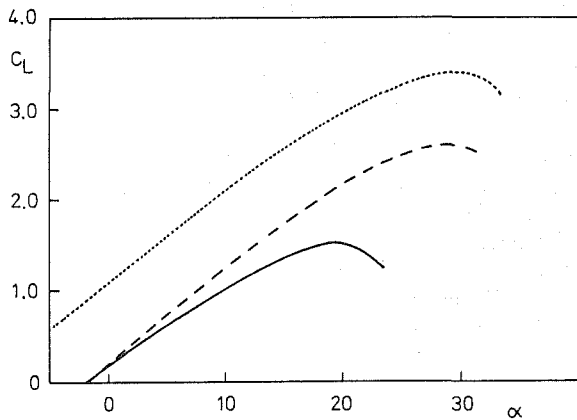


FIGURE 9. Lift curves of an airplane in clean (continuous line), take-off (dashed line) and landing (dotted line) configurations.

advantages regarding simplicity, usage of variables and parameters that are compatible with other parts of the whole method and an acceptable level of accuracy. The downwash angle is computed as

$$e = e_o + \frac{d\epsilon}{d\alpha} \alpha + \Delta e_f \quad (11)$$

where the first right hand term (that depends on the lift distribution at zero angle of attack) is negligible, the second one is related to the wing-tail plane relative position and main parameters of the wing (aspect ratio, taper, sweep, lift curve slope), while the last one varies almost linearly with the increase in wing lift due to high lift system deployment.

### Results

As a test for evaluating the goodness and accuracy of the method, it has been applied to determine the aerodynamic changes of a medium size, short haul transport aircraft, due to deployment of the high lift system.

Main parameters of the aircraft are: aspect ratio equal to 8, taper ratio close to 0.2, swept angle of the  $c/4$  line equal to  $26.6^\circ$ , minimum drag coefficient of 0.019 and horizontal tail volume coefficient near 1. The wing has an aft loaded airfoil, whose main features are:  $t/c=0.12$ ;  $Cl_{max}=1.5$ ;  $Cl\alpha=0.108 \text{ deg}^{-1}$ ;  $Cd_{min}=0.007$ ;  $Cm_o=-0.1$ .

Most of the computations have been performed assuming that a Fowler flap extends from 10% to 65% of the wing trailing edge half span and a series of slats occupy from 10% to 100% of the leading edge. Moreover, the airplane centre of gravity has been placed in a slightly favourable position.

The effect of the airplane high lift system is clearly shown in Fig. 9. Results corresponding to three different settings are depicted: namely, clean aircraft, take-off and landing; in the two last cases with slats and appropriate deflection angles of Fowler flaps. Although the method is developed to determine changes in the aerodynamic characteristics, features of the clean configuration are quite

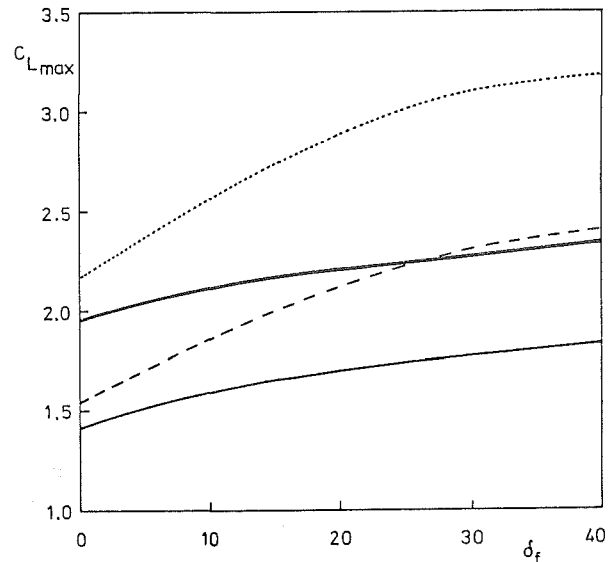


FIGURE 10. Maximum lift coefficient of wing achievable with different high lift device combinations. Plain flap: continuous line; Fowler flap: dashed line; plain flap and slat: solid line; Fowler flap and slat: dotted line.

accurately reproduced too; for example  $Cl_o$  around 0.3 and  $Cl_{max}$  above 1.5. The lift coefficient at angle of attack equal to zero does hardly change when the airplane adopts the take-off configuration due to the opposite effect of leading and trailing edge devices. The maximum lift coefficient increases by an amount of 0.9, mainly due to a slight increase in the lift curve slope and a noteworthy delay of the stall angle. For landing, the airplane has an extra of 1.4 in  $Cl_{max}$ .

To compare the efficiency of various leading edge-trailing edge device combinations some tests have been performed. An example of the results obtained is depicted in Fig. 10, about which a few comments can be done. The general appearance is as expected; the presence of a slat is more effective with Fowler flap than with plain flap since it allows to keep the gain in  $Cl_{max}$  over a wider range of flap deflection angles. Data of the double slotted flap-slat combination are not shown for clearness of the Figure, but they closely follow the ones corresponding to the Fowler flap-slat setting, having a higher maximum at  $45^\circ$  of flap deflection angle.

The last set of results presented here appears in Fig. 11, with the lift over drag ratio of clean, take-off and landing configurations of the airplane. Maxima of  $L/D$  are within the common range of this category of aircraft. Of particular interest is the achievable value of  $L/D$  in take-off setting (above 11.5) because of its relation to second segment climb requirements. As stated in the description of the method, the shape and value of the curves shown near maximum lift are not fully accurate.

### Conclusions

The prediction method described in this paper, developed to determine the aerodynamic characteristics of

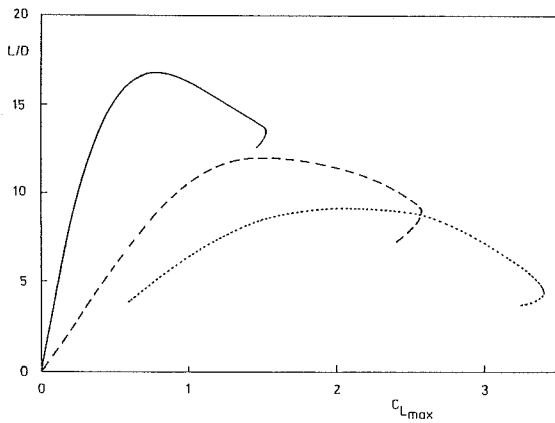


FIGURE 11. Lift over drag ratio curves of complete airplane in clean (continuous line), take-off (dashed line) and landing (dotted line) configurations.

airplanes in low speed configuration, has been proved to perform adequately with a fairly exhaustive series of tests. Although some refinements are still needed, mainly for better adjustments of the parameters of 2D aerodynamics and the 3D stall behaviour, the results obtained indicate that the method is a powerful tool for the preliminary design stage.

#### Acknowledgements

The research in this paper has been partially supported by the Preliminary Design Department of Construcciones Aeronauticas S.A. (CASA) and Universidad Politecnica de Madrid.

#### References

- <sup>1</sup>Sacher, P. W., "Introduction to Special Course on Engineering Methods in Aerodynamics Analysis and Design of Aircraft," AGARD R-783, Jan. 1992, pp. 1.1-1.10.
- <sup>2</sup>McMaster, J. H., and Henderson, M. L., "Some Recent Applications of High Lift Computational Methods at Boeing," *Journal of Aircraft*, Vol. 20, No. 1, Jan. 1983, pp. 27-33.
- <sup>3</sup>Dillner, B., May, F. W., and McMaster, J. H., "Aerodynamics Issues in the Design of High-Lift Systems for Transportation Aircraft," AGARD CP-365, August 1984, pp. 9.1-9.22.
- <sup>4</sup>Murillo, L. E., and McMaster, J. H., "A Method for Predicting Low-Speed Aerodynamic Characteristics of Transport Aircraft," *Journal of Aircraft*, Vol. 21, No. 3, March 1984, pp. 168-174.
- <sup>5</sup>Tinoco, E. N., Ball, D. N., and Rice, F.A., "PAN AIR Analysis of a Transport High-Lift Configuration," *Journal of Aircraft*, Vol. 24, No. 3, March 1987, pp. 181-187.
- <sup>6</sup>Callaghan, J. G., and Beatty, T. D., "A Theoretical Method for the Analysis and Design of Multielement Airfoils," *Journal of Aircraft*, Vol. 9, No. 12, Dec. 1972, pp. 844-848.
- <sup>7</sup>Beatty, T.D., and Naramore, J. C., "Inverse Method for the Design of Multielement High Lift Systems," *Journal of Aircraft*, Vol. 13, No. 6, June 1976, pp. 393-398.
- <sup>8</sup>Hall, I.M., and Suddhoo, A., "Inviscid Compressible Flow Past a Multielement Aerofoil," AGARD CP-365, August 1984, pp. 5.1-5.15.
- <sup>9</sup>Cebeci, T., Chang, K. C., Clark, R. W., and Halsey, N.D., "Calculation of Flow Over Multielement Airfoils at High Lift," *Journal of Aircraft*, Vol. 24, No. 8, August 1987, pp. 546-551.
- <sup>10</sup>Dutt, H. N. V., "Analysis of Multielement Airfoils by a Vortex Panel Method," *AIAA Journal*, Vol. 27, No. 5, May 1989, pp. 658-660.
- <sup>11</sup>Sinhamahapatra, K. P., and Basu, B. C., "Multielement Aerofoils in Viscid Flow," *AIAA Journal*, Vol. 28, No. 5, May 1990, pp. 769-770.
- <sup>12</sup>ESDU, "Increment in Aerofoil Maximum Lift Coefficient due to Deployment of Various High-Lift Devices," ESDU Data Sheets 85033, 1985.
- <sup>13</sup>Roskam, J. *Airplane Design, Part VI: Preliminary Calculation of Aerodynamics, Thrust and Power Characteristics*, Roskam Aviation, Ottawa, Kansas, EEUU, 1987.
- <sup>14</sup>Omar, E., Zierten, T., Hahn, M., Szpiro, E., and Mahal, A., "Two-Dimensional Wind-Tunnel Test of a Nasa Supercritical Airfoil with Various High-Lift System," NASA CR-2215, 1973.
- <sup>15</sup>Condaminas, A., and Becele, J. P., "Determination de l'Effet de Sol sur les Caracteristiques de l'Avion," AGARD 65th Meeting of the Fluid Dynamics Panel, Madrid, Spain, 1989, pp. 24.1-24.12.
- <sup>16</sup>Butter, D. J., "Recent Progress on Development and Understanding of High Lift Systems," AGARD CP-365, August 1984, pp. 1.1-1.26.
- <sup>17</sup>O'Pray, J. E., and Lissaman, P. B. S., "Leading Edge Slat Design by a Semi-Inverse Technique," *Journal of Aircraft*, Vol. 9, No. 2, Feb. 1972, pp. 143-149.
- <sup>18</sup>Ormsbee, A. I., and Chen, A. W., "Multiple Element Airfoils Optimized for Maximum Lift Coefficient," *AIAA Journal*, Vol. 10, No. 12, Dec. 1972, pp. 1620-1624.
- <sup>19</sup>Siladic, M., and Carey, G. F., "Extension of Inverse Design Techniques for Multicomponents Airfoils," *AIAA Journal*, Vol. 26, No. 6, June 1972, pp. 769-770.
- <sup>20</sup>Brune, G. W., and Manke, J. W., "A Critical Evaluation of the Predictions of the NASA-Lockheed Multielement Airfoil Computer Program," NASA CR-145322, 1978.
- <sup>21</sup>Wentz, W. H., "Development of High Lift Flaps and Control Surfaces for New General Aviation Airfoils," NASA CP-2046, 1978, pp. 17-32.
- <sup>22</sup>Porcheron, B., and Thiebert, J. J., "Etude Détaillé de l'Écoulement Autour d'un Profil Hypersustenté. Comparaison avec Calculs," ONERA TP-17, 1984.
- <sup>23</sup>McGhee, R. J., and Beasley, W. D., "Low-Speed Aerodynamic Characteristics of a 17-Percent-Thick Airfoil Section Designed for General Aviation Applications," NASA TN D-7428, 1973.
- <sup>24</sup>Torenbeek, E., *Synthesis of Subsonic Airplane Design*, Delft University Press, Netherland, 1982.
- <sup>25</sup>Goodmanson, L. T., and Gratzer, L. B., "Recent Advances in Aerodynamics for Transport Aircraft," *Astronautics and Aeronautics*, Vol. 11, 1973, pp. 30-45.
- <sup>26</sup>Kohlman, D., *Introduction to V/STOL Aircraft*, Iowa State University, EEUU, 1981.

<sup>27</sup>McRae, D. M., "Aerodynamics of Mechanical High-Lift Devices," AGARD LS-43, 1971, pp. 1.1-1.21.

<sup>28</sup>Boppe, C. W., "Aircraft Drag Analysis Method," AGARD R-783, Jan. 1992, pp. 7.1-7.50.

<sup>29</sup>Multhopp, H., "Methods for Calculating the Lift Distribution of Wings (Subsonic Lifting Theory)," RAE Report Aero 2353, 1950.

<sup>30</sup>Ashley, H., and Landahl, M. L., *Aerodynamics of Wings and Bodies*, Addison-Wesley, Reading 1965, Cap. 7, pp. 129-142.

<sup>31</sup>Cunningham, A. M., "An Efficient, Steady, Subsonic Collocation Method for Solving Lifting Surface Problems," *Journal of Aircraft*, Vol. 8, No. 8, March 1971, pp. 168-176.

<sup>32</sup>Ando, S., and Ichikawa, A., "Quadrature Formulas for Chordwise Integrals of Lifting Surface Theories," *AIAA Journal*, Vol. 21, No. 3, March 1983, pp.466-467.

<sup>33</sup>Schlichting, H., Truckenbrodt, E., and Ramm, H. J., *Aerodynamics of the Airplane*, McGraw-Hill, New York, EEUU, 1979.

<sup>34</sup>McCormick, B. W., *Aerodynamics, Aeronautics and Flight Mechanics*, John Wiley and Sons, New York, EEUU, 1979.

<sup>35</sup>Haftmann, B., Debbeler, F. J., and Gielen, H., "Takeoff Drag Prediction for Airbus A300-600 and A310 Compared with Flight Test Results," *Journal of Aircraft*, Vol. 25, 1988, pp.1088-1096.

<sup>36</sup>Hoerner, *Fluid Dynamic Drag*, Published by de author, 1965.

<sup>37</sup>Oskam, B., Laan, D. J., and Volkers, D. F., "Recent Advances in Computational Methods to Solve the High-Lift Multi Component Airfoil Problem," AGARD CP-365, 1984, pp. 3.1-3.31.